UCRL-PROC-213380

LAWRENCE
LIVERMORE
NATIONAL
LABORATORY

Numerical Modeling of Mixing and Venting from Explosions in Underground Chambers

B. T. Liu, I. Lomov, L. A. Glenn

July 5, 2005

APS Tocial Conference on Shock Compression of Condensed Matter
Baltimore, MD, United States
July 31, 2005 through August 5, 2005

Disclaimer

NUMERICAL MODELING OF MIXING AND VENTING FROM EXPLOSIONS IN UNDERGROUND CHAMBERS

Benjamin T. Liu, Ilya Lomov and Lewis A. Glenn

Energy and Environment Directorate, Lawrence Livermore National Laboratory
7000 East Avenue, Livermore, CA 94550, USA

Abstract. 2D and 3D numerical simulations were performed to study the dynamic interaction of explosion products in an underground concrete chamber with ambient air, barrels of water, and the surrounding walls and structure. The simulations were carried out with GEODYN, a multi-material, Godunov-based Eulerian code that employs adaptive mesh refinement and runs efficiently on massively parallel computer platforms. Tabular equations of state were used to model materials under shock loading. An appropriate constitutive model was used to describe the concrete. Interfaces between materials were either tracked with a volume-of-fluid method that used high-order reconstruction to specify the interface location and orientation, or a capturing approach was employed with the assumption of local thermal and mechanical equilibrium. A major focus of the study was to estimate the extent of water heating that could be obtained prior to venting of the chamber. Parameters investigated included the chamber layout, energy density in the chamber and the yield-to-water mass ratio. Turbulent mixing was found to be the dominant heat transfer mechanism for heating the water.

Keywords: Shock loading, turbulent mixing.
PACS: 47.40.-x, 47.40.Nm.

INTRODUCTION

The effect of low-yield nuclear weapons in underground chambers has been a topic of increasing public debate [1]. We have undertaken fundamental studies of explosions in underground chambers to determine the extent to which chamber contents are heated by such explosions.

In this work, we focus on the potential heating of water contained in the chamber. We consider several different chamber configurations and explosive yields; a large-scale 3D calculation was run in addition to 2D parameter studies.

PROCEDURE

Two-dimensional calculations were performed for a cylindrical chamber with a height of 4 meters and a radius of 6 meters (452 m^3 volume) containing 4.1 metric tons of water. The chamber was located either 0.5 meters or 6.1 meters (20 feet) below the surface. For the latter case, a 0.229m (9 inch) radius vent hole along the centerline was introduced to approximate leakage from the chamber. We simulated our energetic source by depositing energy into a sphere of iron located in the center of the chamber. The yields corresponded to either 1 kiloton or 40 tons of TNT. Most calculations had a torus of water 3 meters from the center of the chamber (off-axis); a calculation with a cylinder of water on the centerline (on-axis) was also run for comparison. In each case, the mass of the water (4.1 metric tons) corresponds to approximately twenty 55-gallon drums. A 1.5 mm iron liner around the water was used to approximate the steel drums.

A large-scale three-dimensional calculation was also run with a 60x10x10 meter rectangular chamber containing 198 stacked 1-ton barrels of water. No iron liner was used for this calculation because there was not enough refinement to resolve the liner. This source used for this calculation had a yield of 2 kilotons.

In both the 2D and 3D calculations, the material surrounding the chamber was assumed to be concrete modeled as a Mohr-Coulomb porous solid. Tabulated equations of state were used for the air, water, and iron in order to accurately determine temperatures and pressures resulting from extreme shock loadings. The source was modeled as a 50 kg sphere of iron.

The various simulations and their parameters are summarized in Table 1.

Computational Tools

Calculations were performed using GEODYN, a Godunov-based Eulerian code with adaptive mesh refinement capabilities. This parallel code features high-order interface reconstruction algorithms and advanced thermodynamically consistent constitutive models described elsewhere [2] that incorporate many of the salient features of the dynamic response of geologic media.

Turbulent mixing was modeled by assuming instantaneous mixing between air, iron, and water in a given cell. The mixing of gases uses an effective gamma from an ideal gas approximation; this effective gamma is used to calculate the effective pressure and temperature of the gas mixture [3]. The mixing length was assumed to be equal to the cell size: 8 mm in the two-dimensional calculations and 32 mm in the three-dimensional calculation.

TABLE 1. Parameters for bomb in chamber simulations.

CASE		SOURCE	CHAMBER		WATER	
		yield	volume	depth	position	mass
A	2D	1 kiloton	452 m^3	0.5 m	*off-axis, torus*	4.1 tons
B	2D	40 tons	452 m^3	0.5 m	*off-axis, torus*	4.1 tons
C	2D	40 tons	452 m^3	6.1 m	*off-axis, torus*	4.1 tons
D	2D	40 tons	452 m^3	0.5 m	*on-axis, cylinder*	4.1 tons
E	3D	2 kilotons	6000 m^3	0.5 m	*off-axis, barrels*	198 tons

Heating Metrics

Heat can be transferred to the water through one of four mechanisms: conduction, shock heating, radiative transfer, and convection. Over the timescales of interest (at most 100 milliseconds), conduction should have a negligible effect. For this work, we neglected the effect of radiative transfer, noting that this may have a noticeable effect, particularly at higher yields.

In our calculations, we consider only shock heating and convective mixing. We will examine the amount of water heated to two different levels: 650 K (the critical temperature of water) and 2600 K (four times the critical temperature). We will present results in terms of the fraction of water in various temperature ranges ($T \leq 650K$, $650K < T \leq 2600K$, and $T > 2600K$) at any given time. While this does not capture the temperature history of a given mass of water, it provides a compact way of viewing the average heating of the water.

RESULTS AND DISCUSSION

In Fig. 1, the temperature distribution in the water for the 1-kiloton source in Case A (see Table 1) is shown.

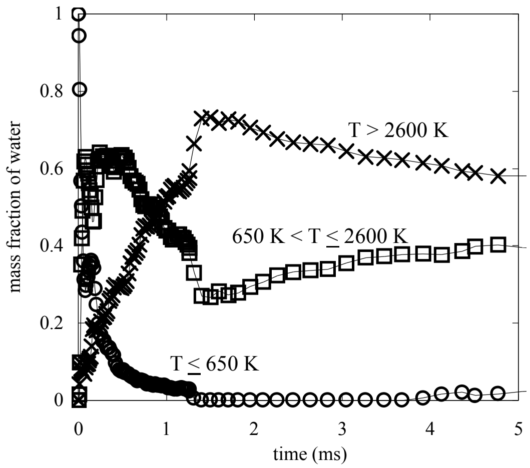

FIGURE 1. Temperature distribution of water for 1-kiloton source and 0.5 m depth-of-burial (Case A from Table 1). The temperature distribution remains approximately constant past 25 ms.

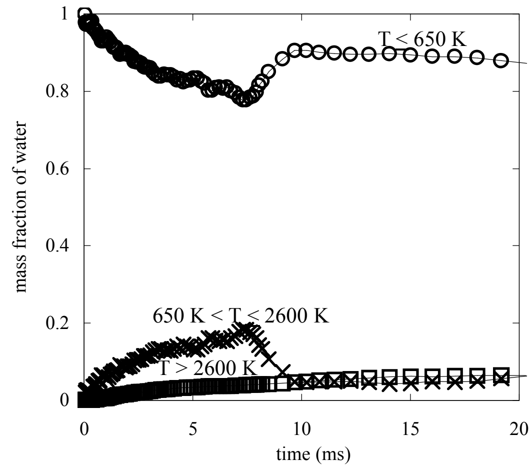

FIGURE 2. Temperature distribution of water for 40-ton source and 0.5 m depth-of-burial (Case B from Table 1). Over 80% of the water remains below 650 K after 40 ms.

Over the first hundred microseconds, the water is rapidly heated by shock heating. Without convective mixing, the water cools as it expands; within 5 ms, almost all the water would be below 373 K. In our case, however, the water is subsequently mixed with the hot air-explosive mixture; this further heats the water and prevents the cooling by expansion. By about one millisecond, over 95% of the water has been heated above 650 K; about half of the water is above 2600 K. The temperature distribution remains approximately the same after 25 ms. Moreover, the remaining 5% of the water stays between 373 K and 650 K and remains within the chamber up to 10 milliseconds, well after the roof has come off.

Fig. 2 shows the analogous simulation for a 40-ton source (Case B). As expected, far less of the water is heated to either 650 K or 2600 K. The majority of the water (almost 80%) is never heated above 650 K.

Venting of Chamber Gases

In measuring the heating of the chamber contents, the time when the contents are vented to the atmosphere is often of great interest. For the 1-kiloton case, the chamber vents in about one millisecond; for the 40-ton case, venting occurs in less than ten milliseconds. In these cases, the water may still be heated after venting as it mixes with the hot gases outside the chamber. In any case, the venting time and the temperature distribution at that time gives some indication of the effectiveness of the heating within the chamber. Table 2 shows the venting time for each case as well as the temperature distribution of the water at the venting time and at 10 ms and 20 ms. In Case C (6.1 m depth-of-burial), hot gas from the explosion escapes very quickly through the vent hole; here we define the venting time as the time when the water first mixes with air initially outside the chamber.

TABLE 2. Venting time and temperature distributions at various times. The venting time for the chamber with a vent hole (denoted with an *) represents the time at which the water first mixes with the atmosphere.

	VENTING				10 ms			20 ms		
CASE	**time**	**≤650 K**	**> 650K ≤2600K**	**>2600 K**	**≤650K**	**> 650K ≤2600K**	**>2600K**	**≤650K**	**> 650K ≤2600K**	**>2600K**
A	1 ms	3%	44%	53%	5%	39%	56%	4%	36%	60%
B	7 ms	78%	18%	4%	90%	5%	5%	87%	6%	7%
C	4 ms*	81%	16%	3%	53%	37%	10%	*Simulation only run to 17.8 ms*		
D	4 ms	37%	48%	15%	46%	32%	22%	54%	24%	22%
E	2 ms	78%	17%	5%	*Simulation only run to 3.7 ms*					

Effect of Source and Chamber Configurations

The yield of the explosive obviously has a strong effect on the temperature distribution in the water, as can be clearly seen by comparing Cases A and B in Figs. 1 and 2, respectively. More important is the ratio of explosive yield to water in the chamber (W/m). Case A has a W/m ratio of about 250 tons/ton, while Cases B, C, D, and E have W/m ratios of about 10 tons/ton. The higher W/m ratio is enough to heat most of the water above the critical point, while the lower value is insufficient to heat all the water above the critical point.

Increased confinement of the explosive gases allows better mixing of the water with the hot gases, resulting in more water heating. This can be seen comparing the temperature distributions in Table 2 for Cases B and C, which differ only by depth-of-burial. Note that the venting time may not necessarily be increased for a deeper chamber if leaks or existing vents are present in the chamber.

Effect of Water Storage Configuration

The location of the water relative to the explosive can have a significant effect on heating of the water. Table 2 shows that when the water is located on-axis (Case D), it experiences significantly more heating than when it is located off-axis (Case B), even though the time to venting is decreased. When the water is closer to the source, it is more thoroughly mixed with the hot explosive gases, resulting in better heating of the water. The specific configuration of the chamber, as well as the accuracy with which the explosive is placed, can greatly influence the effectiveness of the heating.

CONCLUSIONS

This work has examined explosions in shallowly buried chambers and the mixing, heating, and venting of water contained in such chambers. The yield of the explosive relative to the mass of water has the most important effect on the heating of the water. A 1-kiloton explosive with ~4 tons of water (W/m = 250 tons/ton) would heat most of the water above the critical point. With a smaller relative yield (W/m = 10 tons/ton), far less of the water is heated and the specific configuration, including chamber depth-of-burial and the location of the water, becomes more important.

ACKNOWLEDGEMENTS

This work was performed under the auspices of the U.S. Department of Energy by the University of California, Lawrence Livermore National Laboratory under contract No. W-7405-Eng-48.

REFERENCES

1. Nelson, R. W., “Nuclear chamber busters, mini-nukes, and the US nuclear stockpile,” Physics Today, November 2003.
2. Lomov, I. and Rubin, M. B., “Numerical simulation of damage using an elastic-viscoplastic model with directional tensile failure,” Journal de physique iv, vol. 110, pp. 281-286, 2003.
3. Lomov, I. and Liu, B.T., “Approximation of multifluid mixture response for simulation of sharp and diffuse material interfaces on an Eulerian grid,” these proceedings.